

Article

Comparative Study of the Oxidative Degradation of Different 4-Aminobenzene Sulfonamides in Aqueous Solution by Sulfite Activation in the Presence of Fe(0), Fe(II), Fe(III) or Fe(VI)

A. Acosta-Rangel ^{1,2}, M. Sánchez-Polo ¹, M. Rozalen ¹ , J. Rivera-Utrilla ^{1,*}, A.M.S. Polo ¹ and A. J. Mota ¹

¹ Department of Inorganic Chemistry, Faculty of Science, University of Granada, 18071 Granada, Spain; range_432@hotmail.com (A.A.-R.); mansanch@ugr.es (M.S.-P.); marisarozen@ugr.es (M.R.); anisapo@ugr.es (A.M.S.P.); mota@ugr.es (A.J.M.)

² Center of Postgraduate Research and Studies, Faculty of Engineering, University Autonomous of San Luis Potosí, Av. Dr. M. Nava No. 8, San Luis Potosí 78290, Mexico

* Correspondence: jrivera@ugr.es; Tel.: +34-958248523; Fax: +34-958248526

Received: 9 October 2019; Accepted: 3 November 2019; Published: 7 November 2019



Abstract: This study is focused on advanced oxidation technologies (AOTs) using the combined effect of Fe(0–VI)/sulfite systems, that produce mainly $\text{SO}_4^{\bullet-}$ radicals, to remove different 4-aminobenzene sulfonamides (SAs), namely sulfamethazine, sulfadiazine, sulfamethizole, from aqueous solutions. Results obtained showed that neither sulfite nor iron alone is able to degrade SAs; however, the combined effect depends on the oxidation state of iron species whose effectiveness to activate sulfite to promote the degradation of SAs increased following this order: Fe(III) < Fe(II) < Fe(0) < Fe(VI). Using Fe(VI)/sulfite, the complete removal of SAs was obtained in 5 min largely surpassing the effectiveness of the other three systems. The sulfonamides' removal percentage was markedly influenced by sulfite concentration and dissolved oxygen, which improved the generation of oxidant radicals. Response surface methodology was applied, and a quadratic polynomial model was obtained, which allowed us to determine the percentage of SAs degradation as a function of both the iron species and sulfite concentrations. The study of the influence of the water matrix on these AOTs revealed an inhibition of SAs' removal percentage when using ground water. This is probably due to the presence of different anions, such as HCO_3^- , Cl^- , and SO_4^{2-} in relatively high concentrations. According to the byproducts identified, the proposed degradation pathways include hydroxylation, SO_2 extrusion, and different bond-cleavage processes. Cytotoxicity of degradation byproducts, using MTS assay with HEK 293 and J774 cell lines for the first time, did not show an inhibition in cell proliferation, sustaining the safety of the process.

Keywords: advanced oxidation technologies; sulfite; iron; water contaminants; sulfonamides; cytotoxicity

1. Introduction

Several techniques for the treatment of water pollutants by organic compounds, such as biological treatment, adsorption, membrane filtration, traditional and advanced oxidation technologies (AOTs), have been developed in the last decade [1–3]. The AOTs are commonly characterized by the generation of reactive species, including hydroxyl, superoxide, and sulfate radicals, as well as singlet oxygen, and have proven to be highly efficient degrading organic pollutants [4–6].

Sulfonamides (SAs) are synthetic antibiotics that have been widely used as antimicrobial drugs for more than 70 years, and their main advantages are high efficacy, low cost, and broad antibacterial spectrum [7,8]. Therefore, they are used in formulated feed, aquaculture, to prevent the growth of bacteria, and to treat animal infections from some microorganisms and protozoa. SAs have been detected in various municipal sewage treatment plants, hospital effluents, surface water, and even drinking water [9,10]. Although the measured concentration of SAs in different aquatic environments usually maintains at the nanograms per liter to the negative one to micrograms per liter to the negative one levels, which cannot directly shows toxicity or side effects on human health [11], these antibiotics cannot be effectively removed by conventional treatment methods (usually exhibit a low removal rate between 20% and 30%) owing to their implicit antibacterial behavior [12–14]. To control the concentration of SAs in aquatic environments, a potential pathway to eliminate aqueous sulfonamides could be advanced oxidation technologies [15].

Sulfate radical ($\text{SO}_4^{\bullet-}$) is a strong one-electron oxidant with a redox potential ranging from 2.5 to 3.1 V in a wide pH. The redox potential of $\text{SO}_4^{\bullet-}$ is higher than that of a great number of oxidants, as HO^{\bullet} (1.8–2.7 V), and its longer lifetime allows it to react effectively with target organic pollutants. The $\text{SO}_4^{\bullet-}$ lifetime ($3\text{--}4 \times 10^{-5}$ s) is higher than that for HO^{\bullet} (2×10^{-8} s) and, therefore, $\text{SO}_4^{\bullet-}$ has a greater chance to react with organic chemicals. $\text{SO}_4^{\bullet-}$ could be produced through the activation of peroxydisulfate (PDS) and peroxymonosulfate (PMS) by photo-radiation, heat, organic compounds, or transition metals [16–20]. Nevertheless, the use of PDS or PMS in water treatments could be limited due to their elevated cost and residual peroxide species.

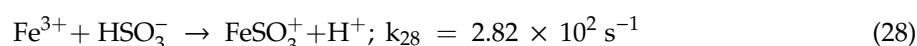
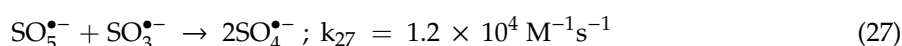
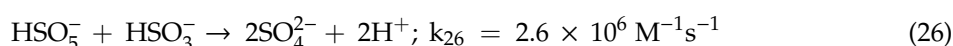
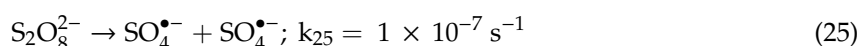
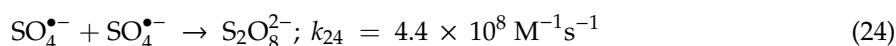
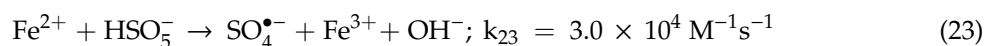
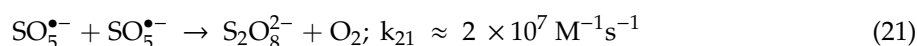
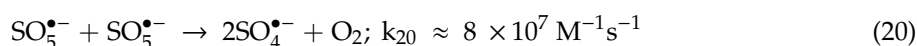
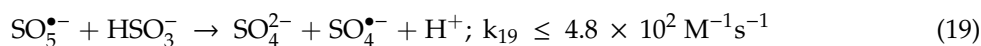
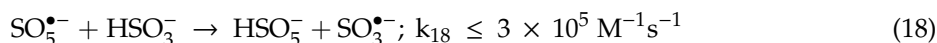
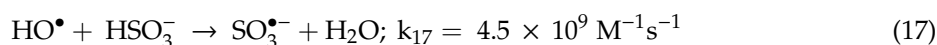
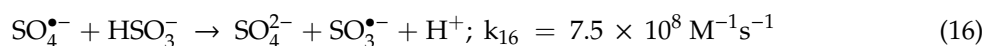
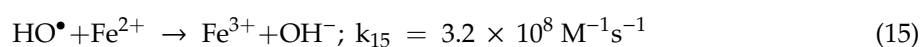
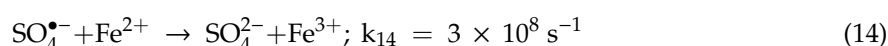
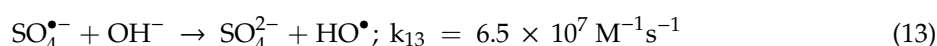
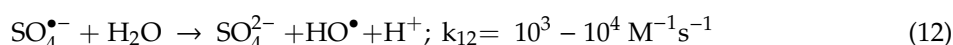
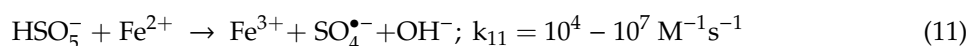
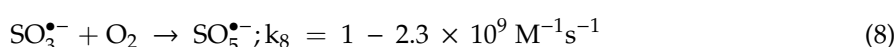
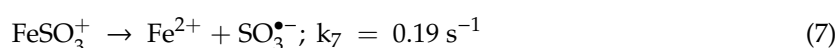
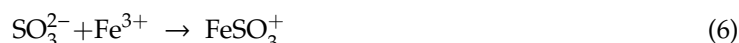
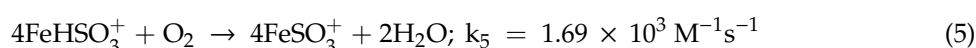
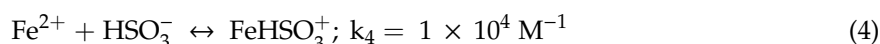
Recent studies have used Fe(0) [21], Fe(II) [22,23], Fe(III) [24–26], and Fe(VI) [27,28] to activate sulfite and successfully produce $\text{SO}_4^{\bullet-}$ to remove organic pollutants. Sulfites are frequently used as food preservatives to prevent microbial spoilage in industry [28]. Due to its low cost, non-toxicity, convenient operation, and high efficiency, the combined process of sulfite and iron-based materials represents potential outstanding methods for producing efficient degrading $\text{SO}_4^{\bullet-}$ radicals [29].

For instance, the Fe(0)/sulfite system degraded brilliant red X-3B azo-dye (80%) with 0.5 and 1.0 mM of Fe(0) and sulfite, respectively. Bicarbonate and halide anions inhibited the removal percentage, and the presence of oxygen was essential to produce $\text{SO}_4^{\bullet-}$ [21]. Sulfamethoxazole (SMX) has also been removed using a Fe(0)/bisulfite/ O_2 system [30]. The results obtained showed a lineal increase in the SMX removal rate as Fe(0) concentration increased with an optimal ratio of Fe(0)/bisulfite concentration of 1:1.

With the Fe(II)/sulfite system, the decolorization of orange II was limited (only 15% reduction) at pH 6.1 within 60 min [23]. Meanwhile, other studies demonstrated the success of the Fe(II)/sulfite system versus the Fe(II)/persulfate and Fe(II)/ H_2O_2 systems decolorizing dyes mix [22]. Concerning the Fe(III)/sulfite system, Zhou et al. [25] demonstrated that approximately 50% of acid orange 7 dye was decomposed within 20 min at pH 3. In addition, As(III) could be oxidized to As(V) using an Fe(III)/sulfite system under visible light, generating free radicals (HO^{\bullet} , $\text{SO}_4^{\bullet-}$, and $\text{SO}_5^{\bullet-}$) [24]. The photo Fe(III)/sulfite system was also efficient at degrading bisphenol A around neutral pH [31]. Guo et al. [29] demonstrated the effective degradation (90%) of 2,4,6-trichlorophenol within 180 min at pH 4 by the UV/Fe(III)/sulfite system.

On the other hand, Fe(VI) alone is a powerful oxidant [32] and, in combination with sulfite, enhances the generation of oxidizing species. Within the Fe(VI)/sulfite system, an emerging contaminant, namely *N,N*-diethyl-3-toluamide (DEET), was degraded at 78% in 10 s, and it was also observed that the presence of humic acid, Cl^- , and $\text{HCO}_3^-/\text{CO}_3^{2-}$ inhibited the oxidation of DEET [27]. Zhang et al. [28] demonstrated the efficiency of the Fe(VI)/sulfite system to degrade a pollutant mixture in 30 s at pH 9.0, whereas Fe(VI) alone only achieved less than 6% removal. Sulfamethoxazole (5 μM), included in this mixture, was degraded at 70% with $[\text{Fe(VI)}] = 50 \mu\text{M}$ and $[\text{sulfite}] = 250 \mu\text{M}$ at pH 9.0 in 30 min. Feng et al. [33] showed accelerated ferrate oxidation of trimethoprim (TMP), enhancing the oxidation to 100% with the addition of one-electron and two electron transfer reductants (SO_3^{2-} and $\text{S}_2\text{O}_3^{2-}$).

According to the above references [22–26], the reactions involved in iron/sulfite complex systems can be resumed as follows (Reactions (1)–(28)):



The use of Fe(II)-Fe(III)/sulfite systems are, therefore, good candidates for their use in the detoxification of contaminated water [22–30,32,34]. Fe(0) represents an alternative as an activator in radicals generation [35], and the use of Fe(VI) and sulfite produces a synergic effect, speeding up the removal of contaminants [28]. The effectiveness of a degradation process in water treatment also implies that the degraded byproducts do not harm the environment. In this context, most toxicological

studies have used *Vibrio fischeri* bacteria tests [16,36], although the application of line cells is becoming more relevant as toxicity models in humans [37].

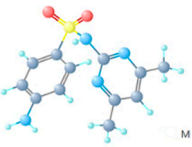
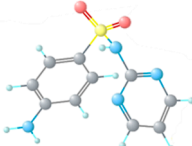
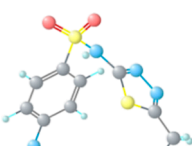
According to this background, AOTs were applied in the present study to degrade three different 4-aminobenzene sulfonamides (sulfamethazine, sulfadiazine, and sulfamethizole) by sulfite activation in the presence of Fe(0), Fe(II), Fe(III), or Fe(VI). As far as we know, this is the first time that these systems of water treatment are used to degrade the above sulfonamides. Thus, the main objectives were (i) to compare the treatment efficiencies of each system for sulfonamide removal; (ii) to investigate the effects of some operational conditions, such as sulfite concentration, iron concentrations, initial pH, and water matrix; (iii) to model the sulfonamide degradation increasing process optimization by response surface methodology (RSM); (iv) to identify the byproducts obtained and investigate the mechanism for sulfonamide degradation in these systems, and (v) to determine the cytotoxicity of the degradation products resulting from each system studied by application of line cells.

2. Materials and Methods

2.1. Materials

All chemicals used in this study, namely sulfamethazine (SMZ) (>99%), sulfadiazine (SDZ) (>99%), sulfamethizole (SML) (>99%), Fe(0) (>95%), ferrous sulfate (>99%), ferric sulfate (>95%), potassium ferrate (>90%), sodium sulfite (>95%), hydroxylamine hydrochloride (NH₂OH·HCl) (99%), hydrochloric acid (pure grade), sodium hydroxide (pure grade), and *tert*-butyl alcohol (>99%), were of analytical grade and supplied by Sigma–Aldrich, Merck KGaA, Darmstadt, Germany. All the solutions were prepared using ultrapure water obtained in an equipment Milli-Q[®] (Milli-pore). Some selected chemical properties of the SAs are shown in Table 1.

Table 1. Molecular structure and physicochemical properties of the 4-aminobenzene sulfonamides used in this study.

Sulfonamide	Molecular Structure (3D)	Molar Mass (g/mol)	LogK _{ow} ^a	Solubility ^b (mg/L)	pK _a
Sulfamethazine C ₁₂ H ₁₄ N ₄ O ₂ S (SMZ)		278.33	0.19	1500 (29 °C)	pK _{a1} : 2.00 pK _{a2} : 6.99
Sulfadiazine C ₁₀ H ₁₀ N ₄ O ₂ S (SDZ)		250.278	−0.09	77 (25 °C)	pK _{a1} : 2.01 pK _{a2} : 6.99
Sulfamethizole C ₉ H ₁₀ N ₄ O ₂ S ₂ (SML)		270.33	0.54	1050 (37 °C)	pK _{a1} : 1.95 pK _{a2} : 6.71

^a Octanol/water partition coefficient; ^b Water solution.

2.2. Experimental Procedure

The SAs degradation experiments with sulfite and different iron species [Fe(0), Fe(II), Fe(III), and Fe(VI)] were conducted in a cylindrical glass reactor with 1 L capacity. Most of the experiments were performed at pH 3 to guarantee the maximum concentration of radicals in the medium and, in the case of Fe(III), to avoid its precipitation. pH media were adjusted by the addition of HCl and NaOH (2N) as required in each case. SAs were first mixed with sulfite in constant agitation at room

temperature (298 K), followed by the addition of different iron species. An initial sample was extracted to verify the initial concentration, and consecutive samples were withdrawn along time. One milliliter of hydroxylamine hydrochloride (1000 mg L^{-1}) was added to quench the reaction. The samples were analyzed after centrifuging at 12,000 rpm for 10 min (Eppendorf Centrifuge 5424) to avoid sampling of possible iron oxide or hydroxide precipitates. Reaction follow-up time was set at 60 min. All samples were preserved in cold storage for further analysis. All experiments were carried out in triplicate.

2.3. Iron-Based/Sulfite Systems

To study the influence of the experimental variables, experiments were conducted by changing the iron species ($1.79 \times 10^{-2} \text{ M}$) from Fe(0) to Fe(VI), whereas the sulfite and SAs concentrations were fixed at 5×10^{-3} and $5.38 \times 10^{-5} \text{ M}$, respectively, also considering either the presence or absence of dioxygen for the Fe(0)/sulfite system. The influence of iron species concentration ($5.37 \times 10^{-4} \text{ M}$ – $1.79 \times 10^{-3} \text{ M}$) was studied with initial concentrations for SAs and sulfite of $5.38 \times 10^{-5} \text{ M}$ and $6.25 \times 10^{-5} \text{ M}$, respectively, whereas the influence of sulfite concentration ($3.12 \times 10^{-3} \text{ M}$ – $6.25 \times 10^{-5} \text{ M}$) was performed using $5.38 \times 10^{-5} \text{ M}$ of SAs and $1.79 \times 10^{-3} \text{ M}$ for the corresponding iron species. In addition, considering the different iron species dominant at pH 3, we determined the SAs reaction rate constants as a function of the reaction rates observed in each case, according to the following Equation (29):

$$k_{\text{obs}} = k[\text{Fe}(n)] \quad \text{being } n = 0, \text{ II, III or VI} \quad (29)$$

where k_{obs} is the reaction rate observed and corresponds to the slope of the straight line obtained when $\text{Ln}(C/C_0)$ (C and C_0 are the final and initial SAs concentrations, respectively) is plotted against the reaction time, k (min^{-1}) is the reaction rate constant with the different iron species, and $[\text{Fe}(n)]$ is the initial concentration of the iron species added in each case. Iron and sulfonamide concentrations were chosen accordingly to properly follow the experiments and also improve their reproducibility.

2.4. Analytical Methods

2.4.1. Fe (VI) Determination in Aqueous Solution

The Fe(VI) concentration was determined using a UV-1600PC Spectrophotometer to ensure the stability of the standard solution, as mentioned by other authors [38]. The calibration curve was obtained with different Fe(VI) concentrations (1–50 ppm) obtained from a potassium ferrate stock solution (500 ppm). The absorbance was measured at a maximum absorption wavelength of $\lambda_{\text{max}} = 510 \text{ nm}$.

2.4.2. Determination of Sulfonamides in Aqueous Solution

SAs concentration was determined by reverse-phase high-performance liquid chromatography (HPLC), using a liquid chromatographer (Thermo-Fisher, Pittsburgh, USA) equipped with UV-visible detector and automatic autosampler with capacity for 120 vials. A PHENOMENEX Kinetex C_{18} column was used ($4.6 \times 150 \text{ mm}$, $2.6 \mu\text{m}$ particle size). The mobile phase was 70% formic acid/ H_2O solution (0.1%, v/v) and 30% acetonitrile in isocratic mode at a flow of 0.35 mL min^{-1} . The detector wavelength was set at 270 nm.

2.4.3. Determination of Byproducts Degradation

Degradation byproducts were identified by using an Acquity ultra-pressure liquid chromatographer (UPLC) (Waters) equipped with a CORTECS™ C_{18} column ($2.1 \times 75 \text{ mm}$, $2.7 \mu\text{m}$) (Waters). The mobile phase in gradient mode (Baseline: 0% B, T8: 95% B, T8.1: 0% B) was Channel A, water with 0.1% formic acid and Channel B, acetonitrile with 0.1% formic acid, at a flow of 0.4 mL min^{-1} . Injection volume was $10 \mu\text{L}$ and column temperature $40 \text{ }^\circ\text{C}$. The UPLC system was coupled to an SYNAPT G2 HDMS Q-TOF high-resolution mass spectrometer (Waters) equipped with electrospray

ionization (ESI) source. Analysis parameters were determined in positive ionization mode, acquiring spectra in a mass range (m/z) between 50 and 1200 amu.

2.4.4. Determination of Byproducts Cytotoxicity

Degradation byproduct cytotoxicity was evaluated by using an MTS assay to determine the viability percentage of human embryonic kidney cells (HEK-293) and J774.2 cell line from BALB/C monocyte-macrophage provided by the CIC cell bank of the University of Granada. A number of 10,000 HEK-293 or J774.2 cells were incubated for 24 h, subsequently changing the medium and adding the SAs 60 min degraded samples; after incubation for 24 h more, 20 μ L of MTS tetrazolium dye was added, and the absorbance at 490 nm was measured after 2 h using an INFINITENANOQUA, reading a given sample 9 times. All experiments were conducted in duplicate.

2.4.5. Collection and Characterization of Natural Waters

Groundwater (GW) and surface water (SW) were collected from well water and a river in Granada (Spain). The samples were characterized following the procedure mentioned elsewhere [36], filtrated, and cold-stored until used. The more representative parameters, namely pH, total organic carbon (TOC), and the concentration of anions (Cl^- , NO_3^- , SO_4^{2-} , and HCO_3^-) were measured.

3. Results and Discussion

3.1. Sulfonamide Degradation by the Fe(0)/Sulfite System

Table S1 (Supplementary Material) shows the results obtained for the Fe(0)/sulfite system at different concentrations of Fe(0) and sulfite. The degradation was negligible for the three SAs used when Fe(0) or sulfite alone were employed for a reaction time of 60 min. However, in the presence of both species together, the degradation percentages for SMZ, SDZ, and SML were 56.3%, 59.1%, and 62.1%, respectively (Table S1, Exp. 10, 20, and 30). These experiments were conducted with the same concentration of Fe(0) and sulfite. Therefore, differences in degradation percentage obtained can be attributed to differences in the molecular structure of the different SAs used.

The effect of sulfite concentration on SAs degradation showed that, for a fixed concentration of Fe(0) of 1.79×10^{-3} M, an increase in sulfite dose from 6.25×10^{-5} M to 3.12×10^{-3} M also led to an increase of 15%, 35%, and 30% in the SMZ, SDZ, and SML degradation, respectively (Table S1, Exp. 6–9, 16–19, and 26–29). The increase in the degradation of SAs by increasing sulfite concentration could be attributed to the contribution of $\text{SO}_3^{\bullet-}$ radicals ($E^\circ = +0.73$ V) and other secondary species, including $\text{SO}_5^{\bullet-}$, $\text{SO}_4^{\bullet-}$, and HSO_5^- formed through Reactions (1)–(10).

The effect of Fe(0) concentration on SAs degradation showed that, for a fixed sulfite concentration of 6.25×10^{-4} M, an increase in Fe(0) concentration considerably increased the SAs degradation. For instance, for SDZ, an increase from 21.6% to 41.4% in its degradation was observed for Fe(0) concentrations of 5.37×10^{-4} and 1.79×10^{-3} , respectively (Table S1, Exp. 14 and 18).

To verify the role of dissolved molecular oxygen in SAs degradation, we selected the system Fe(0)/sulfite. The SMZ degradation kinetics obtained the Fe(0)/sulfite couple was conducted using deoxygenated (nitrogen-purged) and naturally oxygenated (non-purged) water. Figure 1 depicts the results obtained at pH 3. In deoxygenated water, SMZ can be degraded by only 10%; this value is much lower than that obtained when the process was carried out in oxygenated water (56.3%). Consequently, the key role of dioxygen during the degradation process is then confirmed. Previous studies found that Fe(0) in the presence of dioxygen in acidic media can generate reactive species, such as HO^\bullet radicals, and ferrate through Reactions (30)–(33) [39]. At the same time, the sulfate radical can react with water to form HO^\bullet (Reaction (34)).



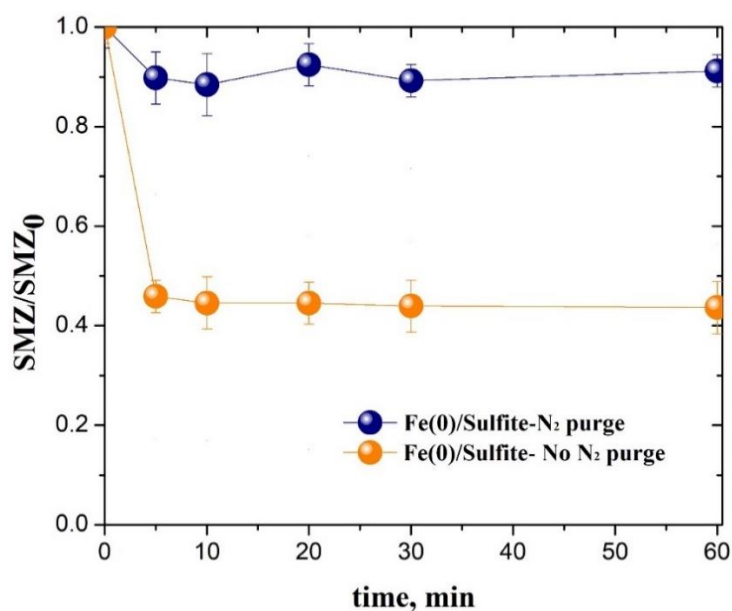
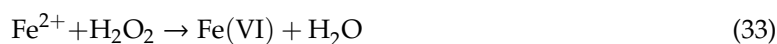


Figure 1. Degradation kinetics of sulfamethazine (SMZ) using the Fe(0)/sulfite system either in the presence or the absence of dioxygen. $[\text{SMZ}] = 5.38 \times 10^{-5} \text{ M}$, $[\text{Fe(0)}]_0 = 1.79 \times 10^{-2} \text{ M}$, $[\text{sulfite}] = 5.0 \times 10^{-3} \text{ M}$, pH 3, T = 298 K.

3.2. Sulfonamide Degradation by the Fe(II)/Sulfite System

To investigate the degradation of SAs in aqueous solution by the Fe(II)/sulfite system, several experiments were carried out at pH 3 varying the dose of Fe(II) and sulfite (Table S2). It was found that Fe(II)/sulfite system can achieve good oxidation of all SAs by means of FeSO_3^+ species (Reactions (5), (6), and (28)) (Table S2, Exp. 39, 48, and 57), since Fe(II) could be easily oxidized to Fe(III) in the presence of O_2 (Reactions (5) and (35)).



On the other hand, in the presence of an excess of sulfite, the rapid formation of Fe(III) is followed by a slower redox process, during which Fe(II) oxidation is independent of its concentration [40]. $\text{SO}_3^{\bullet-}$ radicals, which could be produced by Fe(II) and Fe(III) reaction with sulfite (Reactions (4)–(28)), should then raise the sulfonamide degradation.

3.3. Sulfonamides Degradation by the Fe(III)/Sulfite System

Degradation of SAs by the Fe(III)/sulfite system is shown in Table S3. Comparing SDZ, SMZ, and SML degradations for different conditions, SDZ is the most recalcitrant and is only degraded 28.0% (Table S3, Exp. 75). Fe(III) first serves as a coordinating metal cation leading to the formation of the FeSO_3^+ complex with SO_3^{2-} , and as a radical initiator for $\text{SO}_3^{\bullet-}$, $\text{SO}_5^{\bullet-}$, and $\text{SO}_4^{\bullet-}$ accompanied by the generation of Fe(II) [29]. The continuous generation of $\text{SO}_4^{\bullet-}$ and HO^\bullet is largely subject to the cyclic redox process of Fe(II)/Fe(III) (Reactions (4)–(23)) [34], and could not be studied separately. Wang et al. [41] indicated that the rapid conversion of Fe(II) to Fe(III) limits the ultimate oxidizing capability. Consequently, the Fe(III) concentration has a significant influence on the degradation of SAs (Table S3).

3.4. Sulfonamides Degradation by the Fe(VI)/Sulfite System

Results shown in Figure 2 pointed out that the degradation rate of Fe(VI)/sulfite system is not only the highest but also the more efficient compared with the other studied systems. Indeed, SAs can be degraded in the first 5 min. Owing to, in acidic media, the redox potential of Fe(VI) species ($E^\circ = +2.20$ V) is the highest of the common oxidants used in water treatment [42–45]. To determine the efficiency of Fe(VI)/sulfite system on the SAs degradation, several experiments were carried out (Table S4), concluding that sulfite could be activated by Fe(VI) to completely degrade sulfonamides. For instance, for a fixed Fe(VI) concentration (1.79×10^{-2} M), an increase in the sulfite concentration from 5×10^{-3} to 1×10^{-2} M (Table S4, Exp. 92–93), enhanced the degradation percentage from 83.1% to 100%.

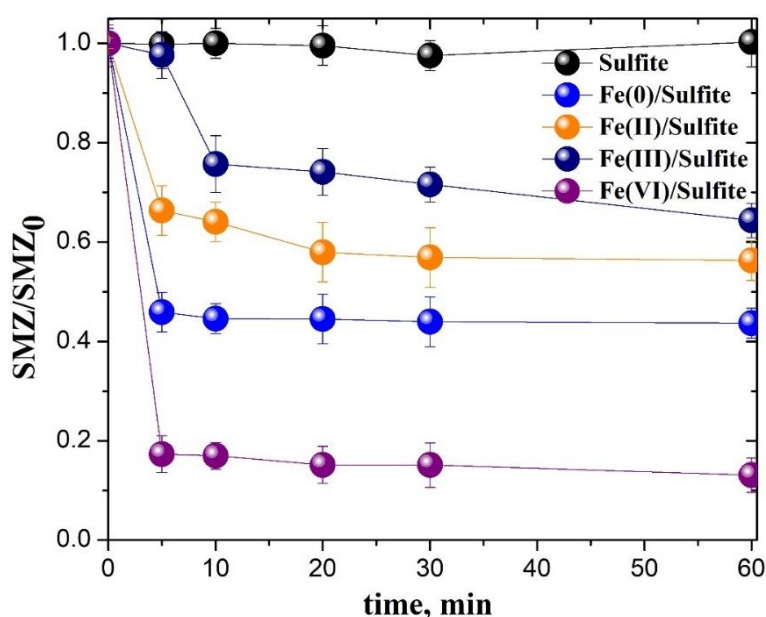
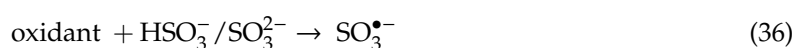
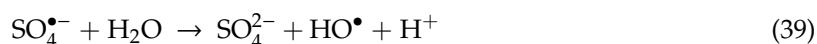
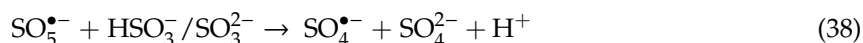


Figure 2. Degradation kinetics of SMZ as a function of the iron-based system used. Initial conditions: $[\text{SMZ}] = 5.38 \times 10^{-5}$ M, $[\text{Fe(0)}]_0 = [\text{Fe(II)}]_0 = [\text{Fe(III)}]_0 = [\text{Fe(VI)}]_0 = 1.79 \times 10^{-2}$ M, $[\text{sulfite}] = 5.0 \times 10^{-3}$ M, pH 3, T = 298 K.

3.5. Comparison of Different Iron-Based/Sulfite Systems on the SAs Removal

To verify the feasibility of Fe(0–VI)/sulfite systems as degradation agents for sulfonamides, sulfamethazine (SMZ) was used as a model compound. The oxidation of SMZ by sulfite in the presence of iron along its different oxidation states is shown in Figure 2. In the sole presence of sulfite, the removal of SMZ observed is negligible. In most systems, the maximum degradation is almost achieved within 10 min, and a very rapid degradation occurred in the first 5 min of reaction. After 60 min of reaction, the degradation percentages were 56.3%, 43.7%, 35.7%, and 86.9% for Fe(0)/sulfite, Fe(II)/sulfite, Fe(III)/sulfite, and Fe(VI)/sulfite, respectively. Consequently, the Fe(VI)/sulfite one presents the greatest removal and, moreover, it is considered as a green oxidant for water and wastewater treatment [42,43]. The redox potential of Fe(VI) is significantly higher (+2.20 V) in an acid medium than in an alkaline medium (+0.72V) [44]; thus, under the studied pH (pH 3), $\text{SO}_4^{\bullet-}$ can be produced through a process similar to Reactions (36)–(38) [45]. Thus, $\text{SO}_3^{\bullet-}$ generated combines with oxygen to form $\text{SO}_5^{\bullet-}$ (Reactions (8)–(9)) that enables the formation of $\text{SO}_4^{\bullet-}$. The formed $\text{SO}_4^{\bullet-}$ quickly reacts with water to produce hydroxyl radicals through Reaction (39).





Among the reasons mentioned above (Section 2.2), we have also selected pH 3 in all experiments because, from Fe(0) at acidic conditions in dioxygen atmosphere, Fe(II) is generated, which is quite stable under these conditions [46,47]. Therefore, the stability of the species Fe(II)/Fe(III), which usually appears cyclically during these reactions, is maintained. Thus, the removal of SMZ could be attributed to the different radical species formed including $\text{SO}_4^{\bullet-}$ ($E^\circ = +2.5\text{--}3.1$ V), $\text{SO}_5^{\bullet-}$ ($E^\circ = +0.81$ V), and $\text{SO}_3^{\bullet-}$ ($E^\circ = +0.73$ V) using Reactions (1)–(12) [48,49]. These results confirmed that sulfite could be activated by iron-based species to accelerate the degradation of recalcitrant contaminants that show a sluggish reactivity with sulfite alone.

3.6. Optimization of SAs Degradation Process Conditions

Response surface methodology (RSM) is an effective method to optimize process conditions, and it can determine the influence of various factors and their interactions on the indexes under investigation (response value) during technological operations. It can be used to fit a complete quadratic polynomial model through a central composite experiment, and it can lead to a more adequate experiment design and result expression [50].

The effect of both sulfite (x) and iron-base (y) concentrations on percentage removal of SAs ($f(x,y)$) was assessed by using a three-level full factorial design with one center point. A total of nine experiments were generated, taking the percentage removal of SAs as response and the concentrations of sulfite and iron-base as independent variables. The experimental responses were fitted to the equations given in Table S5.

Results obtained for our systems showed a similar surface response for the three SAs (SMZ, SDZ, and SML). In Figure 3, as an example, only the Fe(0)/sulfite system is depicted. As it can be seen, the maximum SAs degradation is obtained for concentrations of Fe(0) and sulfite of about 10^{-2} and 5×10^{-3} M, respectively, except for SMZ, for which the slope rises with the sulfite concentration without presenting a maximum in the range of the examined concentrations. The response surfaces for the rest of the systems, namely Fe(II), Fe(III), and Fe(VI), are depicted in Figures S1–S3 in the Supplementary Material.

From the data, the dependence of SAs degradation percentage with sulfite and iron-based concentration ($f(x,y)$) can be calculated using the equations showed in Table S5, which allow us to improve the design and reaction conditions for any system, for example, determining a desired degradation percentage if necessary.

3.7. Influence of the Water Matrix on Iron-Based/Sulfite Systems

Table 2 shows the chemical composition of the water matrix used in this study, and Figure 4 depicts the SAs degradation by using the different iron-based/sulfite systems and types of water. According to Figure 4, the degradation percentage diminishes for all the iron-based systems following the order UW > SW >> GW. However, whereas there is a slight decrease in the degradation of SAs for the Fe(0)- and Fe(VI)-sulfite systems, this variation is more acute for the Fe(III)-sulfite system. This is due, in part, to the partial precipitation of Fe(III) species at the high pH value observed in the GW matrix (Table 2).

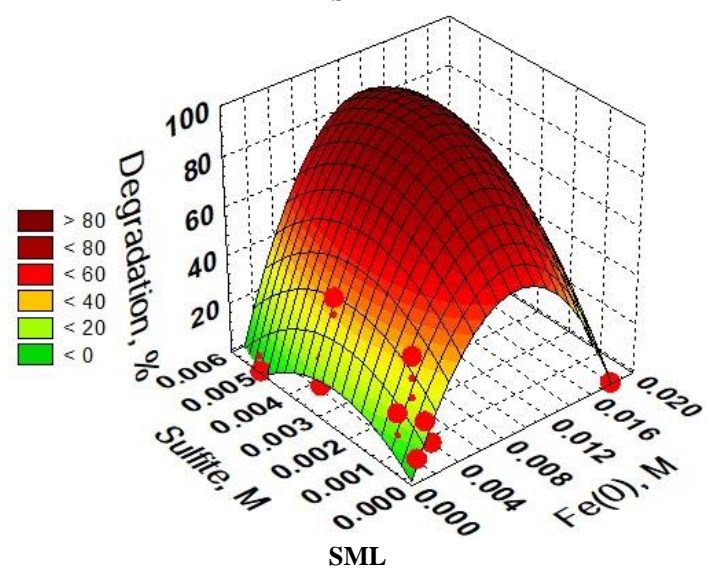
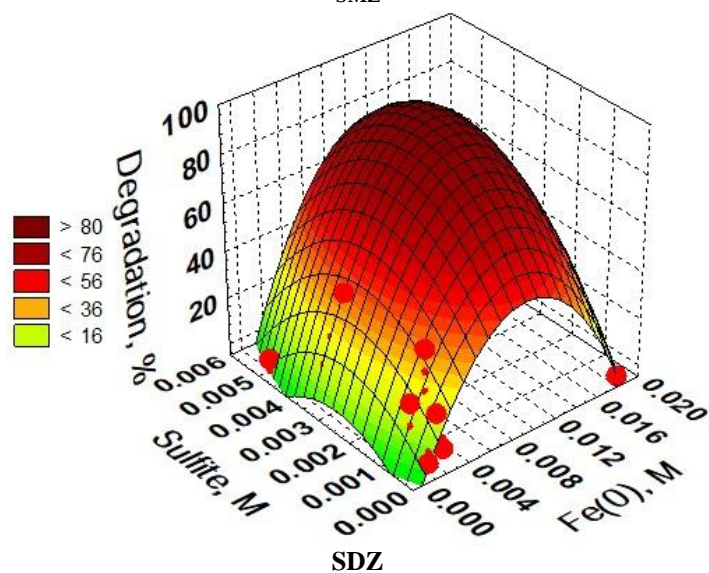
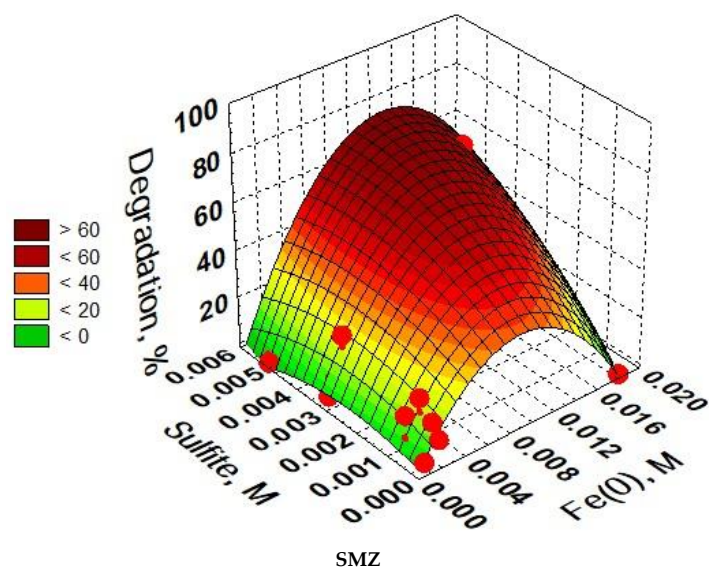
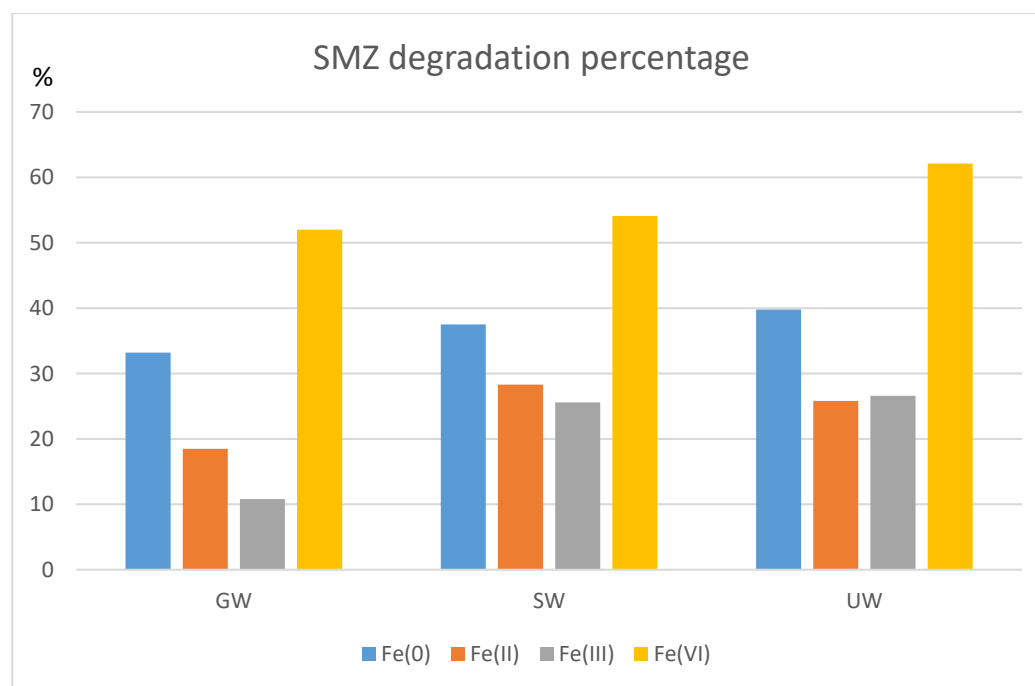


Figure 3. Response surface obtained for the degradation of 4-aminobenzene sulfonamides (SAs) as a function of Fe(0) and sulfite concentrations. [SAs] = 5.38×10^{-5} M, [Fe(0)] = 5.37×10^{-4} – 1.79×10^{-2} M, [sulfite] = 6.25×10^{-5} – 5.0×10^{-3} M, pH 3, T = 298 K.

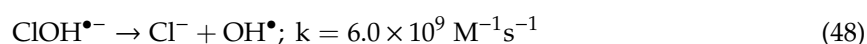
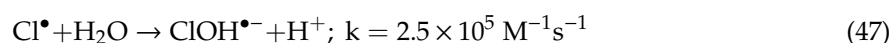
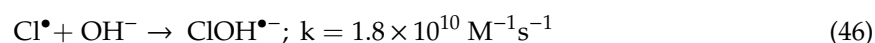
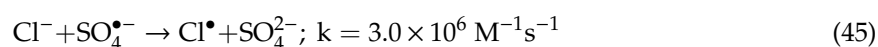
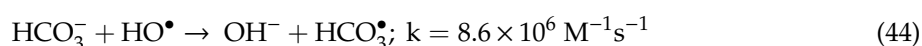
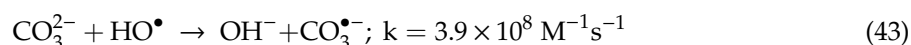
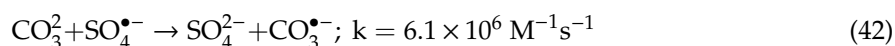
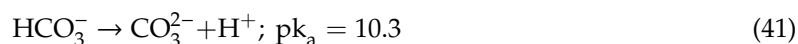
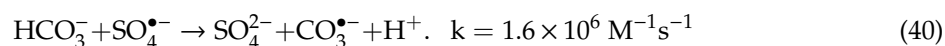
Table 2. Chemical characteristics of the water matrix.

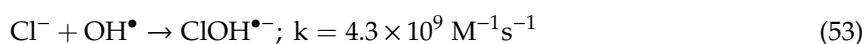
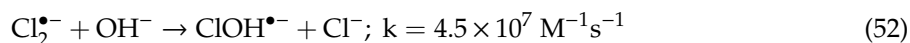
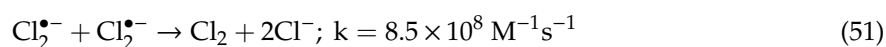
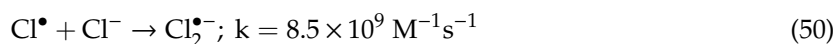
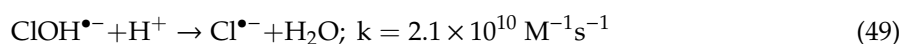
Water	pH	[HCO ₃ ⁻] (mg L ⁻¹)	[SO ₄ ²⁻] (mg L ⁻¹)	[Cl ⁻] (mg L ⁻¹)	[NO ₃ ⁻] (mg L ⁻¹)	TOC* (mg L ⁻¹)
Ultrapure water (UW)	6.8	<BDL	<BDL	<BDL	<DL	<BDL
Surface water (SW)	8.61	143	35.8	<10	2.50	3.5
Ground water (GW)	7.34	156	2404	121	<0.30	2.5

* Total organic carbon.

**Figure 4.** Degradation percentage of SMZ by iron-based/sulfite systems in different water matrixes. [SMZ] = 5.38×10^{-5} M, [Fe(0–VI)] = 1.79×10^{-2} M, [sulfite] = 5.0×10^{-3} M, T = 298 K.

These results can be explained based on the water matrix composition. Thus, the higher concentration of HCO₃⁻, SO₄²⁻, and Cl⁻ in GW could enhance radical scavenging processes (Reactions (40)–(53)) [38,51], diminishing the degradation percentage. However, this diminution is less intense than expected, probably due to new radicals appearing in the scavenging reactions (Reactions (40)–(53)). These secondary radicals, despite being less oxidant, have a longer half-life, which increases their possibility of reaction with pollutant molecules.





3.8. Degradation Byproducts and Pathways

Six major products were found in HPLC/MS analysis after treatment with the iron-based/sulfite systems (Table S6). Owing to the fact that all the systems generate some kind of byproduct, it is more adequate to pay attention to their retention times. Therefore, regarding the retention time (rt) values and correlated masses found, it could be found that lighter degradation compounds were found for SDZ, and the heavier (unique product detected also accompanied by a higher rt value) was found for SML. In principle, this could well correlate with a higher degradation for SDZ, leading to smaller molecules. Casually, among these sulfonamides, SDZ has a simpler structure, which is likely related to its lower resistance against radical attack, given the structural similarities between all of them. Furthermore, the aromatic thiadiazole moiety present in SML is relatively stable in acid media (not in basic solutions) in part due to its π -deficient character that enhances the occurrence of nucleophilic aromatic substitution processes. Thus, detected byproducts ordered by rt were:

(i) From SDZ (molecular mass: 250.28), at 1.14 min, a peak with m/z value of 209.0780 u in full scan positive-mode ESI ($M + \text{H}^+$) was detected, corresponding with a mass of 208.2355 u, meaning a loss of 42 u. Basically, this mass could be assigned to the loss of an oxygen atom of the sulfamide group to give a sulfoxide and the breaking of the pyrimidine moiety to loss two carbon atoms (C_2H_2) followed by a ring-closure to form a diazete moiety (Figure 5).

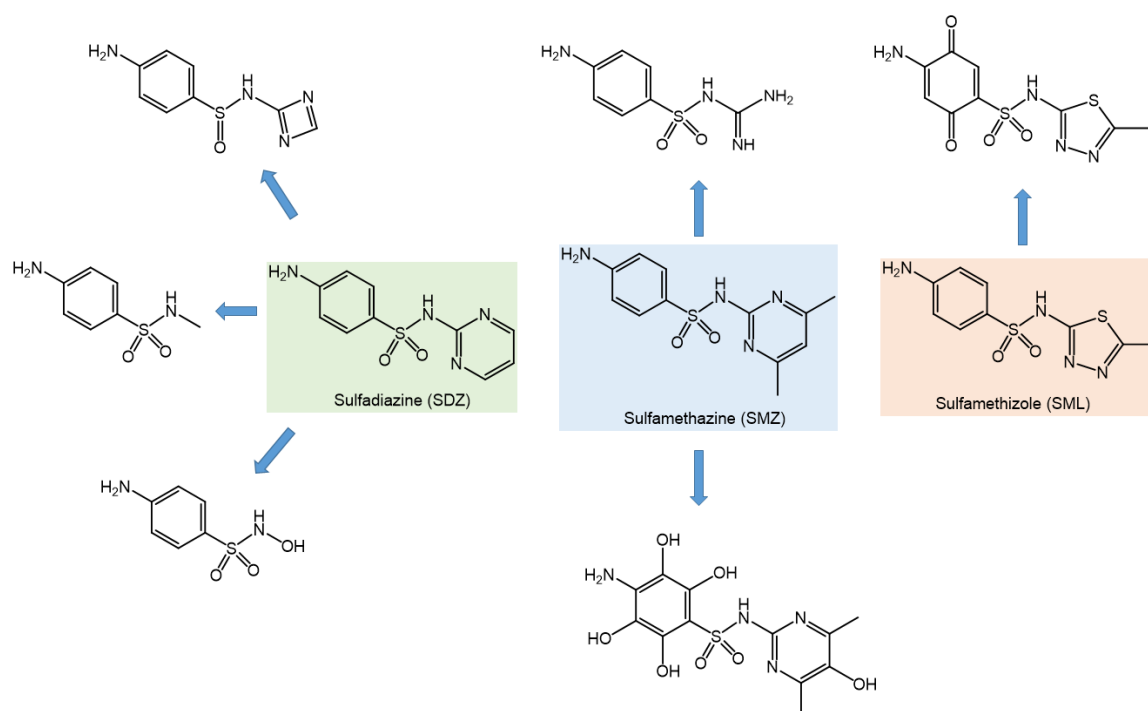


Figure 5. Sulfonamide degradation mechanism through Fe (0-VI)/sulfite systems.

(ii) From SDZ, at 1.90 min, a peak with m/z value of 187.0974 u was detected, corresponding to a mass of 186.2132 u, meaning a loss of 64 u. This mass could be assigned to the loss of SO_2 , which could

be considered as an extrusion-like process, although another likely process consists of the breaking of the pyrimidine moiety to give an *N*-methyl sulfonamide (Figure 5).

(iii) From SDZ, at 3.48 min, a peak with m/z value of 189.1124 u was detected, corresponding to a mass of 188.2291 u, meaning a loss of 62 u. This mass could be assigned to the loss of the pyrimidine moiety and the hydroxylation of the remaining compound to give a hydroxylamine derivative. This nicely explains the high change in the *rt* between this byproduct and the previous case, despite the similar mass between them.

(iv) From SMZ (molecular mass: 278.33), at 3.53 min, a peak with m/z value of 215.1283 u was detected, corresponding to a mass of 214.2664 u, meaning a loss of 64 u. Again, a loss mass that could be assigned to the loss of SO₂, or, more likely, to follow a similar mechanism to the first case involving the breaking of the pyrimidine ring to give a quite stable guanidine moiety (Figure 5).

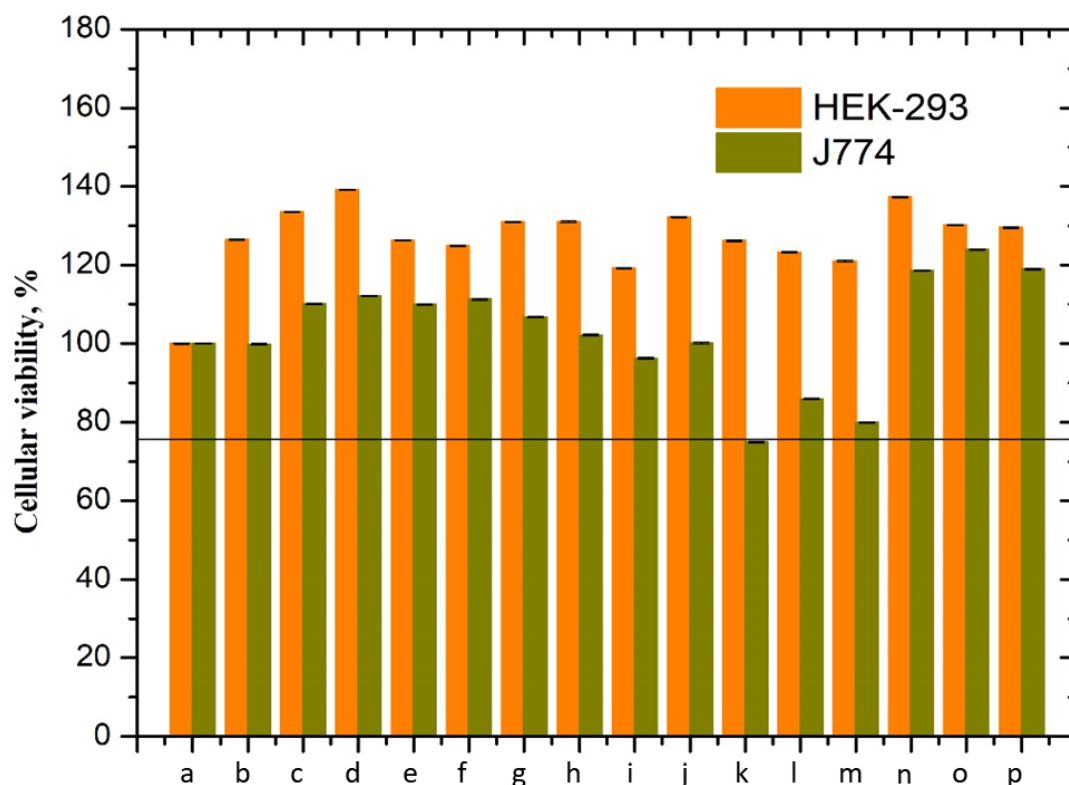
(v) From SMZ, at 3.94 min, a peak with m/z value of 359.0470 u was detected, corresponding to a mass of 358.3934 u, meaning a gain of 80 u, which fairly corresponds to the incorporation of five hydroxyl groups leading to the corresponding perhydroxylated SMZ derivative (Figure 5). This could give us a good indication about the ultimate mechanism operating on these derivatives under experimental conditions, since radical sulfate initiates the radical formation on the aromatic rings of sulfamides as π electrons are energetically more accessible, and, finally, hydroxyl radicals trap these organic radicals leading to the corresponding hydroxylated derivatives.

(vi) From SML (molecular mass: 270.33), at 5.63 min, a peak with m/z value of 301.0067 u was detected, corresponding to a mass of 300.3142 u, meaning a gain of 30 u. As in the previous case, this could be assigned to the incorporation of two oxygen atoms under their carbonyl form, which could be ascribed to the phenyl moiety (in this case the thiadiazole moiety is more stable) in opposite positions to facilitate the electronic delocalization through the corresponding quinonic-like form (Figure 5).

Regarding the different iron-based systems, in the Fe(0), Fe(II), and Fe(III)/sulfite systems, a peak with m/z of 214 was detected at retention time (*rt*) of 3.5 min. These byproducts were commonly founded in degradation systems of SAs as Fenton, UV/persulfate, or gamma irradiation-Fe(II) [52–54].

3.9. Cytotoxicity

Figure 6 shows the percentage of cellular viability of HEK293 and J774 cells as a function of SAs type in different systems. Neither SAs byproducts nor the SAs themselves exhibited inhibition of the growth of human embryonic cells (HEK293) compared to controls (100% of viability). A previous study [55,56] showed that a drug mix, including sulfamethoxazole as SAs, inhibited 30% of HEK293 cell proliferation compared to the control sample. According to the percentage of cellular viability, the byproducts obtained in this study do not present cytotoxicity to cell HEK293. To establish the relative toxicity of SAs compounds, mouse macrophages cells (J774) were also used as a model cell type. The J774 macrophage cell line was chosen due to proven applicability in particulate cytotoxicity and intracellular drug effectiveness studies [57]. For this cell line the percentage cellular viability was less than 75% for the SMZ:Fe(III)/sulfite systems with 74.92% (if the cell viability is less than 75%, the substance is considered to exert a toxic effect on the cells and, if it is greater than 75%, the substance does not exert a toxic effect on the cells). However, most of the byproducts were not cytotoxic to this type of cell, and, therefore, the systems used in this work are viable to use.



(a) Control; (b) SMZ; (c) SDZ; (d) SML
 (e) SMZ/Fe(0)/sulfite; (f) SDZ/Fe(0)/sulfite; (g) SML/Fe(0)/sulfite
 (h) SMZ/Fe(II)/sulfite; (i) SDZ/Fe(II)/sulfite; (j) SML/Fe(II)/sulfite
 (k) SMZ/Fe(III)/sulfite; (l) SDZ/Fe(III)/sulfite; (m) SML/Fe(III)/sulfite
 (n) SMZ/Fe(VI)/sulfite; (o) SDZ/Fe(VI)/sulfite; (p) SML/Fe(VI)/sulfite

Figure 6. Cellular viability (%) of HEK293 and J774 of SAs (sulfamethazine (SMZ), sulfadiazine (SDZ), and sulfamethizole (SML)) by an iron-based/sulfite system. [SAs] = 5.389×10^{-5} M, [Fe(0–VI)] = 1.79×10^{-2} M, [sulfite] = 5.0×10^{-3} M, pH 3, T = 298 K, time = 60 min.

4. Conclusions

Based on this study, we can conclude that the effectiveness of the iron species to activate sulfite anion to promote the degradation of SAs increased following this order: Fe(III) < Fe(II) < Fe(0) < Fe(VI). In fact, the Fe(VI)/sulfite system showed the highest effectiveness being able to completely degrade SAs in a very short period of time (5 min) at acidic pHs (pH 3).

Iron species with sulfite could subsequently form $\text{SO}_3^{\bullet-}$ which can be converted to $\text{SO}_4^{\bullet-}$ in an oxygen atmosphere. The ability to degrade SAs in deoxygenated water diminishes drastically, confirming oxygen's key role to generate reactive species.

Applying the response surface methodology, we have obtained quadratic equations for the systems studied in this research. This mathematical modeling allows calculating the degradation percentage based on a bidimensional grid containing the doses of iron and sulfite added to the system.

A remarkable influence of the water matrix was observed in this study. Consequently, bicarbonate, halide ions, or sulfate present in wastewater and groundwater were able to inhibit the SAs degradation.

Six major products were identified through HPLC/MS analysis for SMZ, SDZ, and SML. The general oxidation pathways proposed are the elimination of SO_2 , C-N bond cleavage on the aromatic ring, different atomic reorganization processes, and hydroxylation reactions promoted by $\text{HO}\bullet$ radicals. None of these byproducts inhibited the growth of cell lines HEK293 and J774.

Consequently, the proposed system Fe(VI)/sulfite is an economic, readily synthesized, and easily handled material with good properties for utilization in SAs degradation in contaminated water.

Supplementary Materials: The following are available online at <http://www.mdpi.com/2073-4441/11/11/2332/s1>, Figure S1. Response surface obtained for the degradation of SAs as a function of Fe(II) and sulfite concentrations. [SAs] = 5.38×10^{-5} M, [Fe(II)] = 5.37×10^{-4} – 1.79×10^{-2} M, [sulfite] = 6.25×10^{-5} – 5.0×10^{-3} M, pH 3, T = 298 K. Figure S2. Response surface obtained for the degradation of SAs as a function of Fe(III) and sulfite concentrations. [SAs] = 5.38×10^{-5} M, [Fe(III)] = 5.37×10^{-4} – 1.79×10^{-2} M, [sulfite] = 6.25×10^{-5} – 5.0×10^{-3} M, pH 3, T = 298 K. Figure S3. Response surface obtained for the degradation of SMZ as a function of Fe(VI) and sulfite concentrations. [SAs] = 5.38×10^{-5} M, [Fe(VI)] = 5.37×10^{-4} – 1.79×10^{-2} M, [sulfite] = 6.25×10^{-5} – 5.0×10^{-3} M, pH 3, T = 298 K. Table S1. Experimental results obtained for SAs degradation in the system Fe(0)/sulfite. Conditions; [Sulfonamide]₀ = 5.38×10^{-5} M, pH 3, T = 298 K, reaction time 60 min. Table S2. Experimental results obtained for SAs degradation in the system Fe(II)/sulfite. Conditions; [Sulfonamide]₀ = 5.38×10^{-5} M, pH 3, T = 298 K, reaction time 60 min. Table S3. Experimental results obtained for SAs degradation in the system Fe(III)/sulfite. Conditions; [Sulfonamide]₀ = 5.38×10^{-5} M, pH 3, T = 298 K, reaction time 60 min. Table S4. Experimental results obtained for SAs degradation in the system Fe(VI)/sulfite. Conditions; [Sulfonamide]₀ = 5.38×10^{-5} M, pH 3, T = 298 K, reaction time 20 min. Table S5. Quadratic equation representing the variation in percentage removal of SAs (f(x,y)) as a function of sulfite (x) and iron-base (y) concentration by different systems. [SAs] = 5.38×10^{-5} M, [Iron-base] = 5.37×10^{-4} – 1.79×10^{-2} M, [sulfite] = 6.25×10^{-5} – 5.0×10^{-3} M, pH = 3, T = 298 K. Table S6. Proposed degradation byproducts by retention time from the different sulfonamide derivatives.

Author Contributions: Conceptualization, M.S.-P. and J.R.-U.; methodology, M.S.-P. and A.A.-R.; software, A.J.M.; validation, M.R. and A.A.-R.; formal analysis, A.A.-R. and M.S.-P.; investigation, A.A.-R. and A.M.S.P.; resources, M.S.-P.; data curation, A.A.-R. and M.R.; writing—original draft preparation, A.A.-R. and M.R.; writing—review and editing, J.R.-U. and A.J.M.; visualization, M.S.-P.; supervision, J.R.-U.; project administration, M.S.-P.; funding acquisition, M.S.-P. All the authors contributed to technical discussions regarding this research.

Funding: This research was funded by both Ministry of Science and Innovation of Spain, grant number CTQ2016-80978-C2-1-R, and CONACyT (Mexico), grant number 407494.

Acknowledgments: The authors sincerely thank editors and anonymous reviewers for improving the manuscript.

Conflicts of Interest: The authors declare no conflict of interest.

References

- Zhao, L.; Deng, J.; Sun, P.; Liu, J.; Ji, Y.; Nakada, N.; Qiao, Z.; Tanaka, H.; Yang, Y. Nanomaterials for treating emerging contaminants in water by adsorption and photocatalysis: Systematic review and bibliometric analysis. *Sci. Total Environ.* **2018**, *627*, 1253–1263. [[CrossRef](#)] [[PubMed](#)]
- Shi, B.J.; Wang, Y.; Geng, Y.K.; Liu, R.D.; Pan, X.R.; Li, W.W.; Sheng, G.P. Application of membrane bioreactor for sulfamethazine-contained wastewater treatment. *Chemosphere* **2018**, *193*, 840–846. [[CrossRef](#)] [[PubMed](#)]
- Kang, J.; Duan, X.; Wang, C.; Sun, H.; Tan, X.; Tade, M.O.; Wang, S. Nitrogen-doped bamboo-like carbon nanotubes with Ni encapsulation for persulfate activation to remove emerging contaminants with excellent catalytic stability. *Chem. Eng. J.* **2018**, *332*, 398–408. [[CrossRef](#)]
- Acosta-Rangel, A.; Sánchez-Polo, M.; Polo, A.M.S.; Rivera-Utrilla, J.; Berber-Mendoza, M.S. Tinidazole degradation assisted by solar radiation and iron-doped silica xerogels. *Chem. Eng. J.* **2018**, *344*, 21–33. [[CrossRef](#)]
- Velo-Gala, I.; Pirán-Montaño, J.; Rivera-Utrilla, J.; Sánchez-Polo, M.; Mota, A.J. Advanced oxidation processes based on the use of UVC and simulated solar radiation to remove the antibiotic tinidazole from water. *Chem. Eng. J.* **2017**, *323*, 605–617. [[CrossRef](#)]
- Niu, H.; Zheng, Y.; Wang, S.; Zhao, L.; Yang, S.; Cai, Y. Continuous generation of hydroxyl radicals for highly efficient elimination of chlorophenols and phenols catalyzed by heterogeneous Fenton-like catalysts yolk/shell Pd@Fe₃O₄@metal organic frameworks. *J. Hazard. Mater.* **2018**, *346*, 174–183. [[CrossRef](#)] [[PubMed](#)]
- Dmitrienko, S.G.; Kochuk, E.V.; Apyari, V.V.; Tolmacheva, V.V.; Zolotov, Y.A. Recent advances in sample preparation techniques and methods of sulfonamides detection—A review. *Anal. Chim. Acta* **2014**, *850*, 6–25. [[CrossRef](#)]
- Ait Lahcen, A.; Amine, A. Mini-review: Recent advances in electrochemical determination of sulfonamides. *Anal. Lett.* **2018**, *51*, 424–441. [[CrossRef](#)]

9. Yin, R.; Guo, W.; Wang, H.; Du, J.; Zhou, X.; Wu, Q.; Zheng, H.; Chang, J.; Ren, N. Enhanced peroxymonosulfate activation for sulfamethazine degradation by ultrasound irradiation: Performances and mechanisms. *Chem. Eng. J.* **2018**, *335*, 145–153. [[CrossRef](#)]
10. Sabri, N.A.; Schmitt, H.; Van der Zaan, B.; Gerritsen, H.W.; Zuidema, T.; Rijnaarts, H.H.M.; Langenhoff, A.A.M. Prevalence of antibiotics and antibiotic resistance genes in a wastewater effluent-receiving river in the Netherlands. *J. Environ. Chem. Eng.* **2018**, *6*, 898–905. [[CrossRef](#)]
11. Zhang, Q.Q.; Ying, G.G.; Pan, C.G.; Liu, Y.S.; Zhao, J.L. Comprehensive evaluation of antibiotics emission and fate in the river basins of China: Source analysis, multimedia modeling, and linkage to bacterial resistance. *Environ. Sci. Technol.* **2015**, *49*, 6772–6782. [[CrossRef](#)] [[PubMed](#)]
12. Gao, P.; Munir, M.; Xagorarakis, I. Correlation of tetracycline and sulfonamide antibiotics with corresponding resistance genes and resistant bacteria in a conventional municipal wastewater treatment plant. *Sci. Total Environ.* **2012**, *421*, 173–183. [[CrossRef](#)] [[PubMed](#)]
13. Adams, C.; Wang, Y.; Loftin, K.; Meyer, M. Removal of antibiotics from surface and distilled water in conventional water treatment processes. *J. Environ. Eng.* **2002**, *128*, 253–260. [[CrossRef](#)]
14. Wallace, J.S.; Garner, E.; Pruden, A.; Aga, D.S. Occurrence and transformation of veterinary antibiotics and antibiotic resistance genes in dairy manure treated by advanced anaerobic digestion and conventional treatment methods. *Environ. Pollut.* **2018**, *236*, 764–772. [[CrossRef](#)] [[PubMed](#)]
15. Liu, N.; Ding, F.; Weng, C.H.; Hwang, C.C.; Lin, Y.T. Effective degradation of primary color direct azo dyes using Fe⁰ aggregates-activated persulfate process. *J. Environ. Manag.* **2018**, *206*, 565–576. [[CrossRef](#)]
16. Zhang, T.; Dong, F.; Luo, F.; Li, C. Degradation of sulfonamides and formation of trihalomethanes by chlorination after pre-oxidation with Fe(VI). *J. Environ. Sci.* **2018**, *73*, 89–95. [[CrossRef](#)]
17. Pagano, M.; Ciannarella, R.; Locaputo, V.; Mascolo, G.; Volpe, A. Oxidation of azo and anthraquinonic dyes by peroxymonosulphate activated by UV light. *J. Environ. Sci. Health A Tox. Hazard. Subst. Environ. Eng.* **2018**, *53*, 393–404. [[CrossRef](#)]
18. Gao, Y.Q.; Gao, N.Y.; Yin, D.Q.; Tian, F.X.; Zheng, Q.F. Oxidation of the β -blocker propranolol by UV/persulfate: Effect, mechanism and toxicity investigation. *Chemosphere* **2018**, *201*, 50–58. [[CrossRef](#)]
19. Watts, R.J.; Ahmad, M.; Hohner, A.K.; Teel, A.L. Persulfate activation by glucose for in situ chemical oxidation. *Water Res.* **2018**, *133*, 247–254. [[CrossRef](#)]
20. Bao, Y.; Lim, T.T.; Wang, R.; Webster, R.D.; Hu, X. Urea-assisted one-step synthesis of cobalt ferrite impregnated ceramic membrane for sulfamethoxazole degradation via peroxymonosulfate activation. *Chem. Eng. J.* **2018**, *343*, 737–747. [[CrossRef](#)]
21. Xie, P.; Guo, Y.; Chen, Y.; Wang, Z.; Shang, R.; Wang, S.; Ding, J.; Wan, Y.; Jiang, W.; Ma, J. Application of a novel advanced oxidation process using sulfite and zero-valent iron in treatment of organic pollutants. *Chem. Eng. J.* **2017**, *314*, 240–248. [[CrossRef](#)]
22. Chen, L.; Peng, X.; Liu, J.; Li, J.; Wu, F. Decolorization of orange II in aqueous solution by an Fe (II)/sulfite system: Replacement of persulfate. *Ind. Eng. Chem. Res.* **2012**, *51*, 13632–13638. [[CrossRef](#)]
23. Zhang, L.; Chen, L.; Xiao, M.; Zhang, L.; Wu, F.; Ge, L. Enhanced decolorization of orange II solutions by the Fe (II)–sulfite system under xenon lamp irradiation. *Ind. Eng. Chem. Res.* **2013**, *52*, 10089–10094. [[CrossRef](#)]
24. Xu, J.; Ding, W.; Wu, F.; Mailhot, G.; Zhou, D.; Hanna, K. Rapid catalytic oxidation of arsenite to arsenate in an iron (III)/sulfite system under visible light. *Appl. Catal. B Environ.* **2016**, *186*, 56–61. [[CrossRef](#)]
25. Zhou, D.; Yuan, Y.; Yang, S.; Gao, H.; Chen, L. Roles of oxysulfur radicals in the oxidation of acid orange 7 in the Fe (III)–sulfite system. *J. Sulfur Chem.* **2015**, *36*, 373–384. [[CrossRef](#)]
26. Jegatheesan, V.; Pramanik, B.K.; Chen, J.; Navaratna, D.; Chang, C.Y.; Shu, L. Treatment of textile wastewater with membrane bioreactor: A critical review. *Bioresour. Technol.* **2016**, *204*, 202–212. [[CrossRef](#)]
27. Sun, S.; Pang, S.; Jiang, J.; Ma, J.; Huang, Z.; Zhang, J.; Liu, Y.; Xu, C.; Liu, Q.; Yuan, Y. The combination of ferrate (VI) and sulfite as a novel advanced oxidation process for enhanced degradation of organic contaminants. *Chem. Eng. J.* **2018**, *333*, 11–19. [[CrossRef](#)]
28. Zhang, J.; Zhu, L.; Shi, Z.; Gao, Y. Rapid removal of organic pollutants by activation sulfite with ferrate. *Chemosphere* **2017**, *186*, 576–579. [[CrossRef](#)]
29. Guo, Y.; Lou, X.; Fang, C.; Xiao, D.; Wang, Z.; Liu, J. Novel photo-sulfite system: Toward simultaneous transformations of inorganic and organic pollutants. *Environ. Sci. Technol.* **2013**, *47*, 11174–11181. [[CrossRef](#)]

30. Du, J.; Guo, W.; Wang, H.; Yin, R.; Zheng, H.; Feng, X.; Che, D.; Ren, N. Hydroxyl radical dominated degradation of aquatic sulfamethoxazole by Fe⁰/bisulfite/O₂: Kinetics, mechanisms, and pathways. *Water Res.* **2018**, *138*, 323–332. [[CrossRef](#)]
31. Yu, Y.; Li, S.; Peng, X.; Yang, S.; Zhu, Y.; Chen, L.; Wu, F.; Mailhot, G. Efficient oxidation of bisphenol A with oxysulfur radicals generated by iron-catalyzed autoxidation of sulfite at circumneutral pH under UV irradiation. *Environ. Chem. Lett.* **2016**, *14*, 527–532. [[CrossRef](#)]
32. Li, P.; He, X.; Li, Y.; Xiang, G.J. Occurrence and health implication of fluoride in groundwater of loess aquifer in the Chinese loess plateau: A case study of Tongchuan, Northwest China. *Expo. Health* **2019**, *11*, 95–107. [[CrossRef](#)]
33. Feng, M.; Jinadatha, C.; McDonald, T.J.; Sharma, V.K. Accelerated oxidation of organic contaminants by ferrate (VI): The overlooked role of reducing additives. *Environ. Sci. Technol.* **2018**, *52*, 11319–11327. [[CrossRef](#)] [[PubMed](#)]
34. Liu, Z.; Guo, Y.; Shang, R.; Fang, Z.; Wu, F.; Wang, Z. A triple system of Fe (III)/sulfite/persulfate: Decolorization and mineralization of reactive Brilliant Red X-3B in aqueous solution at near-neutral pH values. *J. Taiwan Inst. Chem. Eng.* **2016**, *68*, 162–168. [[CrossRef](#)]
35. Kim, C.; Ahn, J.Y.; Kim, T.Y.; Shin, W.S.; Hwang, I. Activation of persulfate by nanosized zero-valent iron (NZVI): Mechanisms and transformation products of NZVI. *Environ. Sci. Technol.* **2018**, *52*, 3625–3633. [[CrossRef](#)]
36. Velo-Gala, I.; López-Peñalver, J.J.; Sánchez-Polo, M.; Rivera-Utrilla, J. Comparative study of oxidative degradation of sodium diatrizoate in aqueous solution by H₂O₂/Fe²⁺, H₂O₂/Fe³⁺, Fe (VI) and UV, H₂O₂/UV, K₂S₂O₈/UV. *Chem. Eng. J.* **2014**, *241*, 504–512. [[CrossRef](#)]
37. Wang, F.; Gao, F.; Lan, M.; Yuan, H.; Huang, Y.; Liu, J. Oxidative stress contributes to silica nanoparticle-induced cytotoxicity in human embryonic kidney cells. *Toxicol. Vitro.* **2009**, *23*, 808–815. [[CrossRef](#)]
38. Zhang, K.; Luo, Z.; Zhang, T.; Gao, N.; Ma, Y. Degradation effect of sulfa antibiotics by potassium ferrate combined with ultrasound (Fe (VI)-US). *BioMed Res. Int.* **2015**, *2015*, 169215. [[CrossRef](#)]
39. Lee, C.; Keenan, C.R.; Sedlak, D.L. Polyoxometalate-enhanced oxidation of organic compounds by nanoparticulate zero-valent iron and ferrous ion in the presence of oxygen. *Environ. Sci. Technol.* **2008**, *42*, 4921–4926. [[CrossRef](#)]
40. Reddy, K.B.; Van Eldik, R. Kinetics and mechanism of the sulfite-induced autoxidation of Fe (II) in acidic aqueous solution. *Atmos. Environ. Part A* **1992**, *26*, 661–665. [[CrossRef](#)]
41. Wang, S.; Wang, J. Trimethoprim degradation by Fenton and Fe (II)-activated persulfate processes. *Chemosphere* **2018**, *191*, 97–105. [[CrossRef](#)] [[PubMed](#)]
42. Dong, H.; Qiang, Z.; Liu, S.; Li, J.; Yu, J.; Qu, J. Oxidation of iopamidol with ferrate (Fe (VI)): Kinetics and formation of toxic iodinated disinfection by-products. *Water Res.* **2018**, *130*, 200–207. [[CrossRef](#)] [[PubMed](#)]
43. Dubrawski, K.; Cataldo, M.; Dubrawski, Z.; Mazumder, A.; Wilkinson, D.; Mohseni, M. In-situ electrochemical Fe (VI) for removal of microcystin-LR from drinking water: Comparing dosing of the ferrate ion by electrochemical and chemical means. *Water Health* **2018**, *16*, 414–424. [[CrossRef](#)] [[PubMed](#)]
44. Kim, C.; Panditi, V.R.; Gardinali, P.R.; Varma, R.S.; Kim, H.; Sharma, V.K. Ferrate promoted oxidative cleavage of sulfonamides: Kinetics and product formation under acidic conditions. *Chem. Eng. J.* **2015**, *279*, 307–316. [[CrossRef](#)]
45. Sharma, V.K. Oxidation of inorganic compounds by ferrate (VI) and ferrate (V): One-electron and two-electron transfer steps. *Environ. Sci. Technol.* **2010**, *44*, 5148–5152. [[CrossRef](#)]
46. Guan, X.; Sun, Y.; Qin, H.; Li, J.; Lo, I.M.; He, D.; Dong, H. The limitations of applying zero-valent iron technology in contaminants sequestration and the corresponding countermeasures: The development in zero-valent iron technology in the last two decades (1994–2014). *Water Res.* **2015**, *75*, 224–248. [[CrossRef](#)]
47. Giannakis, S.; Liu, S.; Carratalà, A.; Rtimi, S.; Bensimon, M.; Pulgarin, C. Effect of Fe(II)/Fe(III) species, pH, irradiance and bacterial presence on viral inactivation in wastewater by the photo-Fenton process: Kinetic modeling and mechanistic interpretation. *Appl. Catal. B* **2017**, *204*, 156–166. [[CrossRef](#)]
48. Neta, P.; Huie, R.E.; Ross, A.B. Rate constants for reactions of inorganic radicals in aqueous solution. *J. Phys. Chem. Ref. Data* **1988**, *17*, 1027–1284. [[CrossRef](#)]

49. Buxton, G.V.; Greenstock, C.L.; Helman, W.P.; Ross, A.B. Critical review of rate constants for reactions of hydrated electrons, hydrogen atoms and hydroxyl radicals ($\cdot\text{OH}/\cdot\text{O}$ in aqueous solution. *J. Phys. Chem. Ref. Data* **1988**, *17*, 513–886. [[CrossRef](#)]
50. Bezerra, M.A.; Santelli, R.E.; Oliveira, E.P.; Villar, L.S.; Escalera, L.A. Response surface methodology (RSM) as a tool for optimization in analytical chemistry. *Talanta* **2008**, *76*, 965–977. [[CrossRef](#)]
51. Yang, Y.; Jiang, J.; Lu, X.; Ma, J.; Liu, Y. Production of sulfate radical and hydroxyl radical by reaction of ozone with peroxymonosulfate: A novel advanced oxidation process. *Environ. Sci. Technol.* **2015**, *49*, 7330–7339. [[CrossRef](#)] [[PubMed](#)]
52. Wan, Z.; Wang, J. Fenton-like degradation of sulfamethazine using $\text{Fe}_3\text{O}_4/\text{Mn}_3\text{O}_4$ nanocomposite catalyst: Kinetics and catalytic mechanism. *Environ. Sci. Pollut. Res.* **2017**, *24*, 568–577. [[CrossRef](#)] [[PubMed](#)]
53. Li, M.; Wang, C.; Yau, M.; Bolton, J.R.; Qiang, Z. Sulfamethazine degradation in water by the VUV/UV process: Kinetics, mechanism and antibacterial activity determination based on a mini-fluidic VUV/UV photoreaction system. *Water Res.* **2017**, *108*, 348–355. [[CrossRef](#)] [[PubMed](#)]
54. Batista, A.P.S.; Pires, F.C.C.; Teixeira, A.C.S.C. The role of reactive oxygen species in sulfamethazine degradation using UV-based technologies and products identification. *J. Photochem. Photobiol. A Chem.* **2014**, *290*, 77–85. [[CrossRef](#)]
55. Pomati, F.; Castiglioni, S.; Zuccato, E.; Fanelli, R.; Vigetti, D.; Rossetti, C.; Calamari, D. Effects of a complex mixture of therapeutic drugs at environmental levels on human embryonic cells. *Environ. Sci. Technol.* **2006**, *40*, 2442–2447. [[CrossRef](#)]
56. Cizmas, L.; Sharma, V.K.; Gray, C.M.; McDonald, T.J. Pharmaceuticals and personal care products in waters: Occurrence, toxicity, and risk. *Environ. Chem. Lett.* **2015**, *13*, 381–394. [[CrossRef](#)]
57. Weaver, K.D.; Kim, H.J.; Sun, J.; MacFarlane, D.R.; Elliott, G.D. Cyto-toxicity and biocompatibility of a family of choline phosphate ionic liquids designed for pharmaceutical applications. *Green Chem.* **2010**, *12*, 507–513. [[CrossRef](#)]



© 2019 by the authors. Licensee MDPI, Basel, Switzerland. This article is an open access article distributed under the terms and conditions of the Creative Commons Attribution (CC BY) license (<http://creativecommons.org/licenses/by/4.0/>).